JOURNAL OF MECHANICAL ENGINEERING AND SCIENCES (JMES)
ISSN: 2289-4659 e-ISSN: 2231-8380
VOL.14, ISSUE 1, 6488 – 6496
DOI: https://doi.org/10.15282/jmes.14.1.2020.23.0508

ORIGINAL ARTICLE

Experimental and simulation study of mild steel response to lateral quasi-static compression

Omar Abdulhasan Lafta [1*], Minah Mohammed Fareed[1] and Md Radzai Bin Said [2]

[1] Al-Musaib Technical College, Al-Furat Al-Awsat Technical University, Babel, Iraq
[2] Faculty of Mechanical Engineering, Universiti Teknikal Malaysia Melaka, Hang Tuah Jaya, 76100 Durian Tunggal, Melaka, Malaysia.

ABSTRACT – Collision of structure of a vehicle is not limited to the axial direction but it can occur laterally. The purpose of this paper is to present a study of the energy absorption behavior of different length of the circular mild steel tube under lateral crushing. A ring/tube (length of 10 mm, 35 mm, and 60 mm), 60 mm diameter and 1.5 mm thickness is compressed quasi-statically. Maximum loading setup to Instron machine was 50 kN. The speed of compression is 5mm/min. Finite Element Analysis (FEA) it used to validate the experimental work to ensure of getting accurate results. Numerical results of energy absorption and collapse load showed respectively 96.52% and 94.36% agreement with experimental results. The theoretical results showed 14.37% deviation with experimental and 15.5% with numerical results. The specimen with 60 mm length leads to better energy absorption than the other specimens. The results obtained numerically and experimentally in addition to theoretically showed the energy absorbed and collapse load varies with the length of the tube.

ARTICLE HISTORY
Revised: 30th Dec 2019
Accepted: 30th Dec 2019

KEYWORDS
Energy absorption; circular tube; Finite Element; lateral crushing.

INTRODUCTION

Dissipation of impact kinetic energy through tubular structures was the main concern of scientists and designers over more five decades. Energy absorption through plastic deformation of the material is often used particularly in the form of tubular systems. These tubular can be verity to square, hexagon, frusta, circular and honeycomb. These tubular can absorb different amounts of kinetic energy depending on them geometries [1]. It is necessary to investigate energy absorption characteristics and crushed loads to predict the suitable application [2]. Circular ring/tube as example widely used as energy absorber due to low manufacturing cost and high efficiency. Circular ring/tube can absorb various type of energy due to different type of deformation which results various dissipation of kinetic energy. The mechanism of deformation of the tube structure involve lateral indentation and crushing [3], axial crushing with and without hole [4, 5], as well as tube splitting and inversion [6]. The lateral crushing of circular tube was studied by Hodge et al. [1]. The authors used a rigid perfectly plastic mild steel material to predict the force and deformation response. They found the geometry and properties of material are the effects on the collapse load. The lateral crushing of circular mild steel and aluminum tube under quasi-static direction was investigated experimentally and numerically by Gupta et al. [7]. They found the collapse load and energy absorption increases with the decrease of the diameter and increase the thickness of the tube. Numerous researches have studied Aluminum honeycomb empty and foam filled behavior under different loading direction. Hui et al. [8] studied axial and lateral crushing responses of aluminum honeycomb which filled with EPP foam. The influence of filling aluminum honeycomb on the energy absorption was studied by Liu et al. [9]. They found the mechanical performance of aluminum honeycomb filled with circular CFRP tube under axial crushing increases absorbed energy. Later composite material used in energy absorption researches under out-of-plane and in-plane compression tests with different cross-sections and shapes to examine it is ability of absorbing collision energy [10]. Empty and polyurethane foam filled tubes were studied experimentally and theoretically under lateral crushing loading [11]. They calculated theoretically the deformation of empty and foam filled circular composite tube. At present, the researchers have modeled in the finite element analysis to investigate the behavior of deformation of energy absorption systems under quasi-static loading. It is adequate procedure to simulate real experiment to improve the accuracy of design model. Crashworthiness of types composite tubes were examined experimentally and numerically by modeling softwares [12-14].

Nested tubes with varied cross-sections subjected to the lateral quasi static condition were examined experimentally, theoretically by Tran [15], and numerically through commercial ANSYS LSDYNA software by Olabi et al. [16]. The axil crushing of tubular structure have vastly used as energy absorbing devices due to large amount of absorbed energy through plastic deformations. However, these tubular structures have defects due to different types of deformation modes and much high fluctuations of mean load [17]. The benefits of lateral compression of tubular structure are the bending collapse mode which obtained as a deflection due reaction of the applied load, and the stable mode of deformation. Even thought of advantages of lateral compression, these circular structures have limited concern with previous researchers.

*CORRESPONDING AUTHOR | Omar Abdulhasan Lafta | ✉ com.la.omar@atu.edu.iq

In this paper, the effect of mechanical deformation behavior of the different circular length ring/tube of the specimen under quasi-static loading between two rigid platens is investigated. Furthermore, effect of different length of the specimen on the energy absorption during the flattening process are examined in experimental, numerical and theoretical manner.

THEORETICAL WORK

Load Displacement Curve Characteristics

The load-displacement curve is a relationship between the load and displacement obtained after completing one of the compression, tension, shear, bending, and torsion experiments, which explains the mechanical behaviour of the structure. The load-displacement curve provides the information of the elastic region, collapse region, plateau or strain-hardening region and the densification region [18]. Energy absorption considered one of the load- displacement characteristics which defined as the ability of tubular structure to absorb or dissipate the kinetic energy due to the plastic deformation of the tubular structure [19]. The energy absorption of a structure can be measured by integrating area under load-displacement curve [20], as illustrated in Equation. (1).

$$E_{absorbed} = \int p \, d\delta \tag{1}$$

where, $E_{absorbed}$ is the energy absorption (in kJ), P is the compression load (in kN) and δ is the deformation of ring/tube (in metre).

To evaluate the amount of energy absorption theoretically needs to employ trapezoidal rule (Equation. (2)) due to non-liner relationship between load (p) and deformation (δ). Theoretical energy absorption can be calculated after obtaining the equation of load- displacement curve.

$$\int_a^b f(x)dx = (b-a)\left[\frac{f(a)+f(b)}{2}\right] \tag{2}$$

where, a ,b are the distance from (x_1) to (x_2) of load-displacement curve.

Theoretical compression load can be calculated by using Equation. (3):

$$p = \frac{p_o}{\sqrt{1-\left(\frac{\delta}{D}\right)^2}} \tag{3}$$

where, P_o is the initial collapse load (in kN) and D is the diameter of ring/tube (in metre).

Collapse load can be calculated theoretically by using the following formula:

$$p_o = \frac{4M_p}{R} \tag{4}$$

where M_p is the fully plastic bending moment (in kN.m) and R is the radius of ring or tube (in metre).

$$M_p = \frac{\sigma_y * t^2 * h}{4} \tag{5}$$

where σ_y is the yield stress (in MPa), t is the thickness of ring/tube (in metre) and h is the length of ring/tube (in metre).

EXPERIMENTAL WORK

Material Properties

The mild steel used in this paper is a commercial product. All mild steel specimens were manufactured in hot rolled, and the contain of carbon is less than 25%. Tensile test which performed to identify the mechanical properties of the material's specimens. The tension tests of Mild steel specimens were prepared according to ASTM E8/E8M-13a [21]; the thickness: 1.5 mm, width: 12.5 mm, gage length: 50mm and Width of grip section: 20mm.The extensometer was used to determine the displacements of tensile specimens. Figure 1(a) and (b) explains the tensile test of the mild steel specimen.

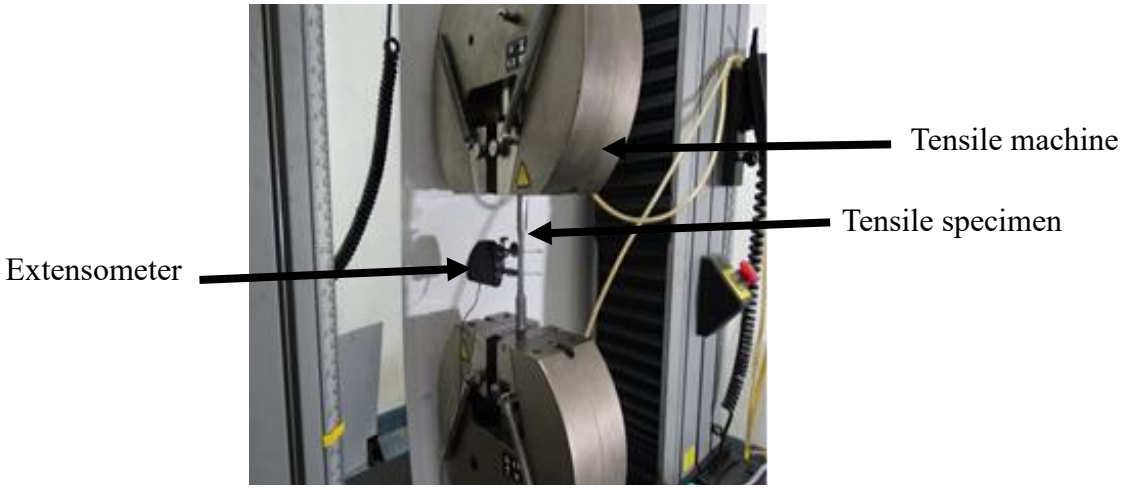

(a)

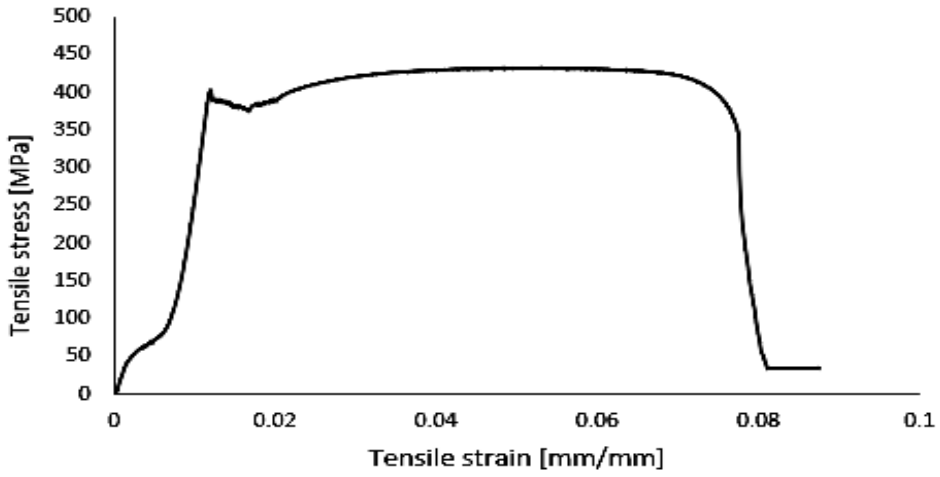

(b)

Figure 1. (a) tensile test experiment and (b) tensile stress-strain curve.

The curve that obtained from tensile test shows nonlinear behavior in the beginning of the elastic region due to using the shell (curvature) tensile specimen even though nocked both of the grips ends of the specimen according to ASTM E8/E8M-13a [21]. The nonlinear behavior continues until obtaining fully straight grips ends of the specimen to start linear deformation until yield point. From tensile curve, it can be seen the flow stress region starts (upper flow stress point) after material yielding due to continuous increasing of stress which leads to: loss in material quality until reach to lower flow stress point, and start with increase crystal dislocation which makes the stress and strain in irregular relationship which takes this region wavy shape.Strain hardening region starts immediately after stress flow region [22]. As a result of increasing stress that leads to increasing crystal dislocations which impede the previous sliding dislocations that make material be harder which requires an increase of the stress to obtain more deformation. Neck region occurs due to increasing of stress with a smaller cross section of material until failure [23]. Table 1 shows the mechanical properties of mild steel.

Table 1. Mechanical properties of circular mild steel.

Density (kg/m^3)	Poisson's ratio	Yield stress (MPa)	Modulus of elasticity (GPa)
7850 [24]	0.3 [25]	378.56	210

Experimental Procedure

All lateral compression experiments were carried out on Instron machine 5585 under quasi-static loading. The loading capability of the Instron machine is 250 kN. Loading cell was used to measure loading force by attaching with the upper cross head (moving head). The maximum load setup to the universal testing machine was 50 kN. The computer that connected with the Instron machine by Bluehill 3 software which used to control the moving head velocity and provide the obtained data during the experiment to the computer. Different parameters can obtain from this test such as energy, compression stress, load,compression strain, displacement and time of compression. The crushing velocity that

programmed to the moving head was 5 mm/min to prevent any dynamic effect. The quasi-static compression test of circular ring/tube under lateral loading with the Instron machine explains in Figure 2.

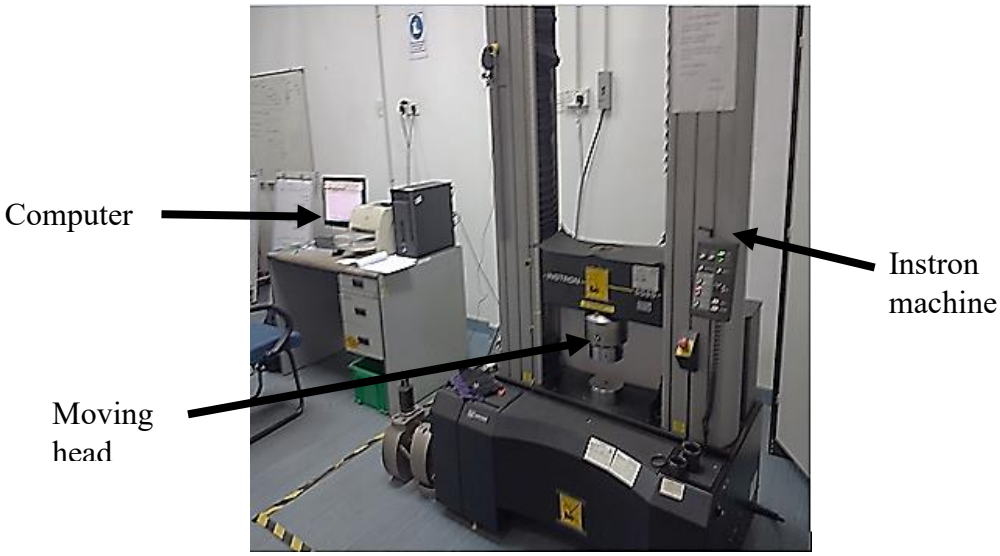

(a)

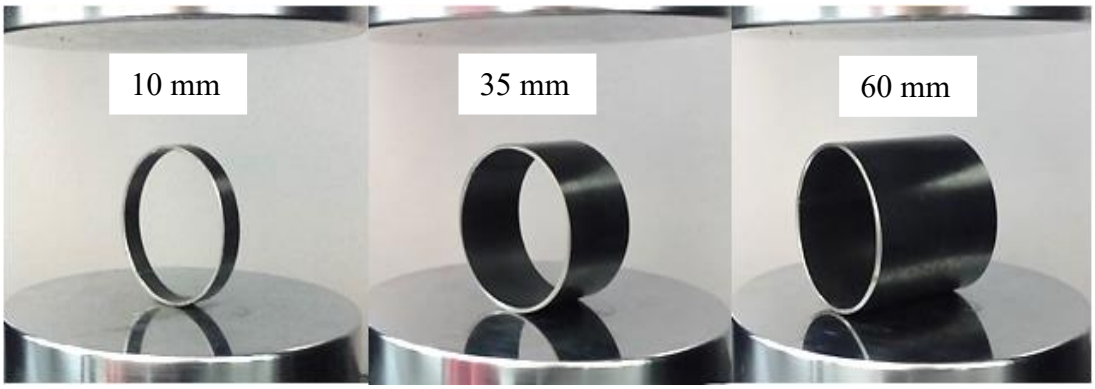

(b)

Figure 2. (a) Instron machine and (b) different length of mild steel specimens.

Mild steel tube with 60 mm diameter and 1.5 mm thickness was used to obtain all of the test specimens with length (10 mm, 35 mm, and 60 mm). During the experiment, all specimens were put in the center of the lower plate (fixed head) to obtain the accurate distribution of the applied load from upper plate (moving cross head) as illustrates in Figure 2.

Numerical Procedure

Numerical finite element analysis were carried out by using Abaqus / standard Explicit Model which contain many capabilities to analyze nonlinear quasi-static analysis. The upper and lower platen of Instron machine had been plotted in ABAQUS package to simulate real compression experiments. Upper plate had been given a velocity to move in negative y-axis (direction of crush) while the lower plate was fixed with all direction. Mesh module from Quad type R3D4 type was used to create finite element on the upper and lower plates, based on assumption that they were discretely rigid to predict the deformation behavior and obtain accurate distribution of load to the specimen. Modeling of ring in ABAQUS was performed by drawing a circle with the same diameter of each experiment. Deformable option was selected to make the ring respond to the load that applied by upper plate. After plotting the circle, it was extruded to the desired lengths of 10 mm, 35 mm, and 60 mm. Interaction module is very important part of the finite element analysis when two or more objects are in contact. Interaction between ring with upper and lower plate was created by identifying type of contact to be generally explicit, which means the contact was just touching without tying between the components of that system. By default, ABAQUS uses a penalty scheme to impose friction constraints for tangential interaction in the contact analysis. The penalty scheme allows some relative motion of the surfaces when it should be sticking. The magnitude of sliding is limited to an elastic slip, which is characterized by slip tolerance and contact surface length. The coefficient of friction 0.2 between system components [26]. The mesh of the ring used in this work was Quade type (S4R) due to choosing the specimens as shell. The small size was inversely proportional with the ring/tube response to the compression load applied from the upper plate and the reaction force that came from the lower plate.

RESULTS AND DISCUSSION

To validate the model of the different length of circular ring/tube that used in this paper the numerical and theoretical results should compare with experimental results. Comparison between experimental, numerical and theoretical results was performed in. load-displacement curve and energy absorption capability. Figure 3 shows the load-displacement curve under quasi-static lateral loading.

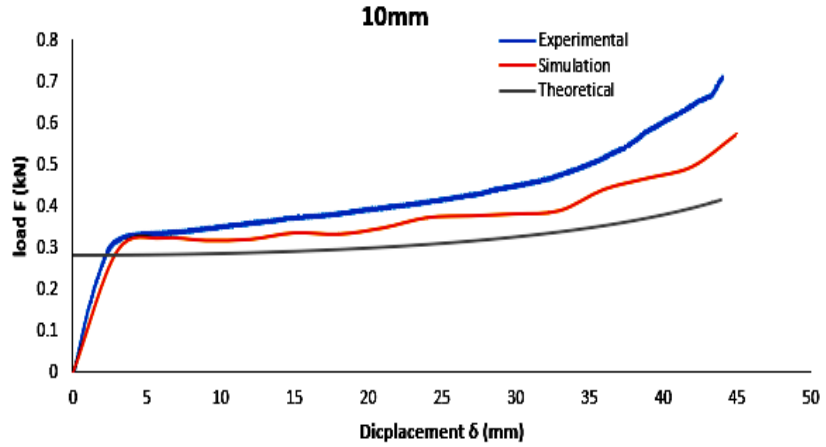

(a)

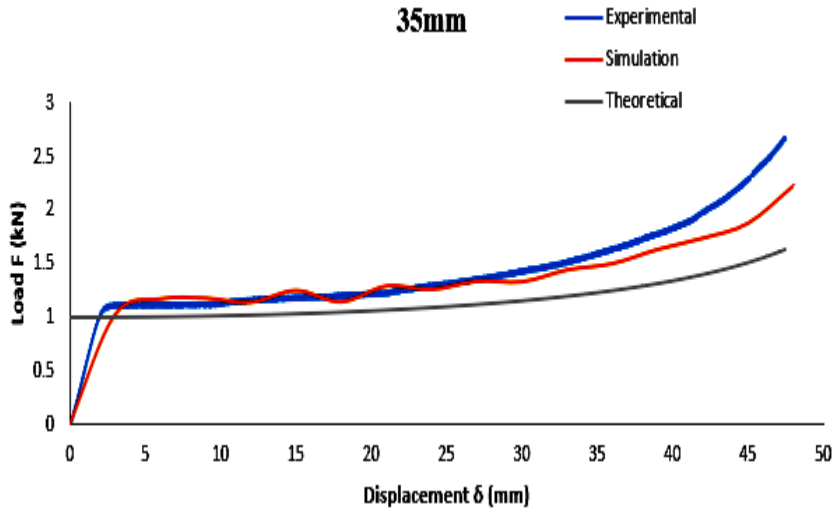

(b)

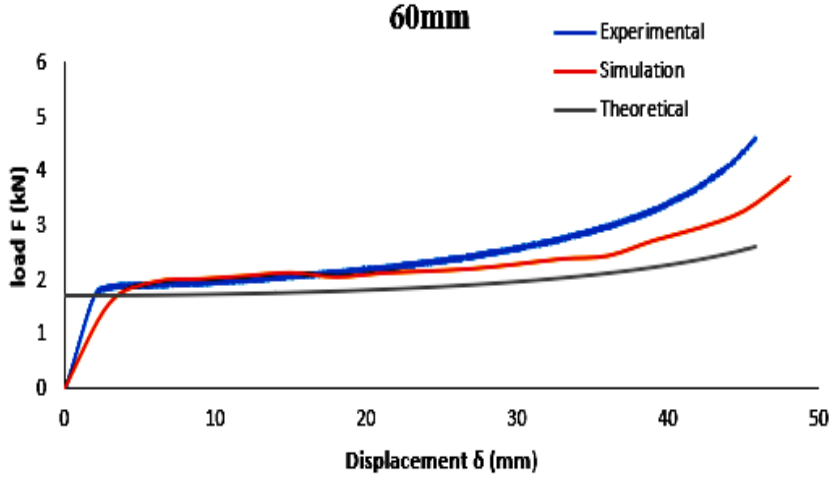

(c)

Figure 3. Comparison between finite element results with the experimental and theoretical results: (a) 10 mm, (b) 35 mm and (c) 60 mm.

It can be clearly seen the results of the finite element for all specimens were reached to 94.36 % (as shown in Tabel 3) agreement (or 5.64% deviation) with the experimental results at collapse load stage followed by a nominal change after collapse stage. This change was explained in stress- strain curve which exhibit flow stress region and strain hardening behavior. Mild steel material cannot be considered as a bilinear material due to points of data generate a slope greater than zero [25]. Then the finite element does not have the accuracy to recognize the flow stress followed by strain hardening phenomenon. The deviation which appears clearly between theoretical and experimental results is 8.7% and 20.03% for collapse load and energy absorption respectively. In addition the deviation between theoretical and numerical is 13.87% and 17.18% for the same previous terms. This devietion is due to the differing behavior of the material during theoretical ,experimental and numerical work.

The differentiates between the experimental, numerical and theoretical results of 10 mm, 35 mm and 60 mm ring/tube specimens (simultaneously) under quasi-static lateral loading were performed in Figure 4.

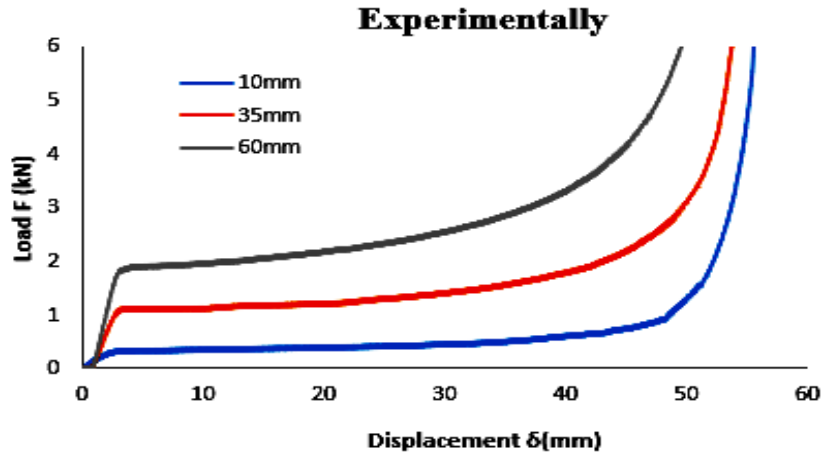

(a)

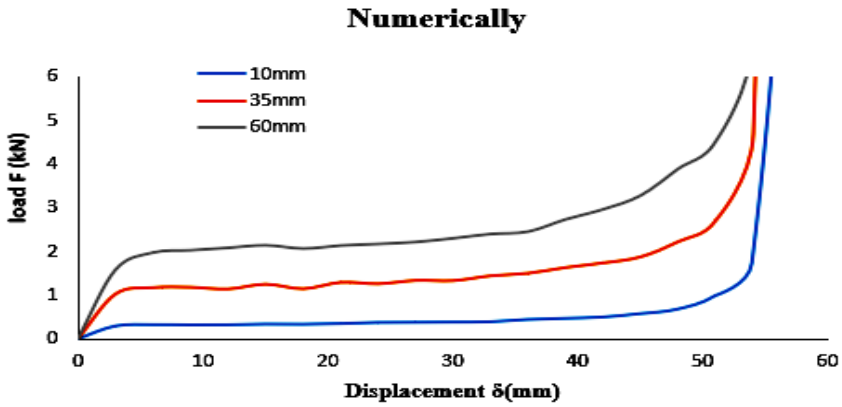

(b)

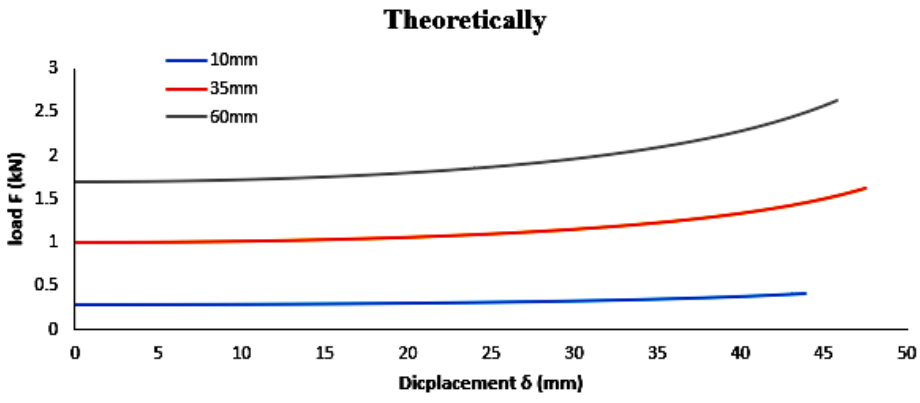

(c)

Figure 4. Load displacement curve of (10, 35 and 60) mm specimens: (a) experimentally (b) numerically and (c) theoretically.

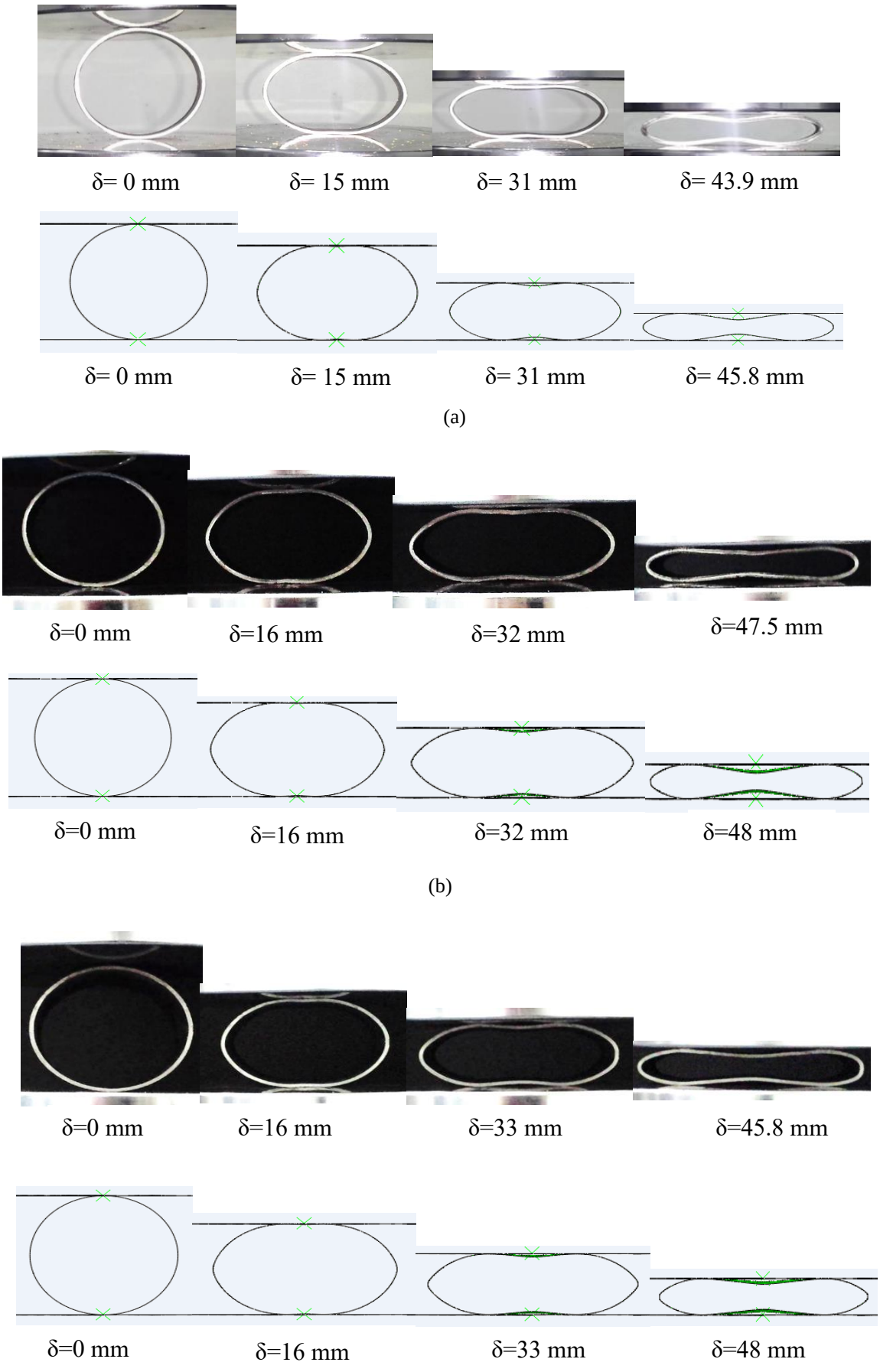

Figure 5. Experimental and numerical deformation history of (a) 10 mm ,(b) 35 mm and (c) 60 mm length specimens.

Figure 3(a) illustrates the load-displacement curve of the specimen with 10 mm length. The deformation of ring started linearly in the elastic region until the collapse at 0.315 kN. Deformation increased gradually with the increase of the load after collapse point, as a result of strain hardening of the mild steel ring. Deformation still increased because of increase of load. The shape of specimen seemed to be elliptical at Figure 5 (a) (δ=15 mm). Due to the increase of load, two small concavities were formed inward of the ring at (δ=31 mm) making elliptical slot between the specimen and each of moving and fixed crosshead. Increase of load seems to continue until complete crushing even when reaching 43.9 mm while numerically the specimen reaches to the densification at 45.8 mm due to tangential friction between specimen and two platens that increase with increases length of the ring. Four plastic hinges could be seen clearly at (δ= 43.9 mm) and the shape of structure formed a shape of two similar adjacent eyes. Figure 5 presented that all different lengths of specimens showed 96.52% agreement between experimental and numerical results. However, the theoretical curve as shown in Figure 3 (a) it 14.37% deviates with experimental due to mild steel material was assumed to be rigid perfectly plastic in theory while in reality the material behaves elastic-strain hardening. The deformation pattern by 35 mm and 60 mm specimens was similar to the 10 mm specimen; however, the difference between them in collapse point position was due to difference in the length of the specimens as shown in Figure 4.

It can be seen clearly from this graph that the increase of the length of specimen led to the increase of collapse load value, which caused the increase of lateral force linearly [27]. This led to the increase the area under the curve that represented energy absorption due to increase of the contact area between the specimen and the upper, lower cross head of the Instron machine. Table 2 illustrates the effect of different length of specimens on collapse load experimentally, numerically and theoretically.

Table 2. Experimental and numerical collapse load with different length specimens.

Term	Length	Experimental (kN)	Simulation (kN)	Theoretical (kN)
Collapse load	10 mm	0.31	0.32	0.28
	35 mm	1.08	1.17	0.99
	60 mm	1.85	1.97	1.7

It can be clearly seen from Figure 4. The variation of the area under the curve (energy absorption) with the length of the ring/tube due to increasing the contact area between the specimen and with the upper, lower flat plate. Table 3. Illustrates the effect of different length of specimens on the energy absorption experimentally and numerically.

Table 3. Experimental and numerical energy absorption with different length specimens.

Term	Length	Experimental (kJ)	Simulation (kJ)	Theoretical (kJ)
Energy absorption	10 mm	18.51	16.93	13.98
	35 mm	65.16	64.22	54.47
	60 mm	109.87	109.36	88.77

CONCLUSION

In this work, mild steel material has been used to examine the effect of different length of ring/tube on the energy absorption and collapse load under quasi-static lateral loading. ABAQUS software based on the dynamic/explicit code has been employed to simulate experimental results. The experimental, numerical and theoretical results showed the following concluding points:

i) The collapse load and energy absorption were varied with the length of ring/tube.
ii) Numerical results showed 96.52% agreement with experimental results in term of energy absorption as well as 94.36% in term of collapse load.
iii) Theoretical results showed 14.37% and 15.5 % deviation with the experimental and numerical results respectively.

This deviation is due to different behavior of mild steel through theoretical, experimental and numerical work. Generally increasing the length of the specimen leads to increase the value of collapse load and energy absorption of all specimens during experimental, numerical and theoretical results.

REFERENCES

[1] DeRuntz Jr JA, Hodge Jr PG. Crushing of a tube between rigid plates. Journal of Applied Mechanics. 1963;30:391-395.

[2] Hussein RD, Ruan D, Lu G, Guillow S,Yoon JW. Crushing response of square aluminium tubes filled with polyurethane foam and aluminium honeycomb. Thin-Walled Structures. 2017;110:140-154.

[3] Huang Z, Zhang X, Zhang H. Energy absorption and optimization design of multi-cell tubes subjected to lateral indentation. Thin-Walled Structures. 2018;131:179-191.

[4] Fareed MM, Lafta OA, Said MR. The axial crushing of circular tube under quasi static loading. Journal of Engineering and Applied Sciences. 2017;12:4818-4823.

[5] Eyvazian A, Tran TN, Hamouda AM. Experimental and theoretical studies on axially crushed corrugated metal tubes. International Journal of Non-Linear Mechanics. 2018;101:86-94.

[6] Reddy TJ, Narayanamurthy V, Rao YVD. Evolution of a new geometric profile for an ideal tube inversion for crash energy absorption. International Journal of Mechanical Sciences. 2019;155:125-142.

[7] Gupta NK, Sekhon GS, Gupta PK. Study of lateral compression of round metallic tubes. Thin-Walled Structures. 2005;43:895-922.

[8] Liu Q et al. Axial and lateral crushing responses of aluminum honeycombs filled with EPP foam. Composites Part B: Engineering. 2017;130:236-247.

[9] Wang Z, Liu J. Mechanical performance of honeycomb filled with circular CFRP tubes. Composites Part B: Engineering. 2018;135:232-241.

[10] Alkateb M, Sapuan SM, Leman Z, Jawaid M, Ishak MR. Quasi-static crush behaviour of environmentally friendly kenaf/wool epoxy composites elliptical tube. Journal of Mechanical Engineering and Sciences. 2018;12:3671-3688.

[11] Elahi SA, Rouzegar J, Niknejad A, Assaee H. Theoretical study of absorbed energy by empty and foam-filled composite tubes under lateral compression. Thin-Walled Structures. 2017;114:1-10.

[12] Zhang Z, Sun W, Zhao Y, Hou S. Crashworthiness of different composite tubes by experiments and simulations. Composites Part B: Engineering. 2018;143:86-95.

[13] Supar K, Ahmad H. Multi-holes configurations of woven fabric kenaf composite plates: experimental works and 2-D modelling. Journal of Mechanical Engineering and Sciences. 2018;12:3539-3547.

[14] Rayhan S. A comprehensive study on the buckling behaviour of woven composite plates with major aerospace cutouts under uniaxial loading. Journal of Mechanical Engineering and Sciences. 2019;13:4756-4776.

[15] Tran T. A study on nested two-tube structures subjected to lateral crushing. Thin-Walled Structures. 2018;129:418-428.

[16] Baroutaji A, Gilchrist MD, Olabi AG. Quasi-static, impact and energy absorption of internally nested tubes subjected to lateral loading. Thin-Walled Structures. 2016;98:337-350.

[17] Baroutaji A, Gilchrist MD, Smyth D, Olabi AG. Crush analysis and multi-objective optimization design for circular tube under quasi-static lateral loading. Thin-Walled Structures. 2015;86:121-131.

[18] Movahedi N, Linul E. Quasi-static compressive behavior of the ex-situ aluminum-alloy foam-filled tubes under elevated temperature conditions. Materials Letters. 2017;206:182-184.

[19] Niknejad A ,Rahmani DM. Experimental and theoretical study of the lateral compression process on the empty and foam-filled hexagonal columns. Materials & Design. 2014;53:250-261.

[20] Albahash ZF, Ansari MNM. Investigation on energy absorption of natural and hybrid fiber under axial static crushing. Composites Science and Technology. 2017;151:52-61.

[21] Standard test methods for tension testing of metallic materials ASTM E8 / E8M-13a.West Conshohocken, PA. : ASTM International. 2013.

[22] Davis JR. Tensile testing, 2nd ed. ASM international. 2004.

[23] Garg A, Bhattacharya A. An insight to the failure of FDM parts under tensile loading: finite element analysis and experimental study. International Journal of Mechanical Sciences. 2017;120:225-236.

[24] Adlakha I, Bazehhour BG, Muthegowda NC, Solanki KN. Effect of mechanical loading on the galvanic corrosion behavior of a magnesium-steel structural joint. Corrosion Science. 2018;133:300-309.

[25] Baroutaji A, Morris E, Olabi AG. Quasi-static response and multi-objective crashworthiness optimization of oblong tube under lateral loading. Thin-Walled Structures. 2014;82:262-277.

[26] Guan W, Gao G, Li J, Yu Y. Crushing analysis and multi-objective optimization of a cutting aluminium tube absorber for railway vehicles under quasi-static loading. Thin-Walled Structures. 2018;123:395-408.

[27] Niknejad A, Elahi SA, Liaghat GH. Experimental investigation on the lateral compression in the foam-filled circular tubes. Materials & Design (1980-2015). 2012;36:24-34.